nature medicine

Fetuin-A acts as an endogenous ligand of TLR4 to promote lipid-induced insulin resistance

Durba Pal[1,7], Suman Dasgupta[1,2,7], Rakesh Kundu[1], Sudipta Maitra[1], Gobardhan Das[3], Satinath Mukhopadhyay[4], Sukanta Ray[5], Subeer S Majumdar[6] & Samir Bhattacharya[1,2]

Toll-like receptor 4 (TLR4) has a key role in innate immunity by activating an inflammatory signaling pathway. Free fatty acids (FFAs) stimulate adipose tissue inflammation through the TLR4 pathway, resulting in insulin resistance[1–7]. However, current evidence suggests that FFAs do not directly bind to TLR4[8,9], but an endogenous ligand for TLR4 remains to be identified. Here we show that fetuin-A (FetA) could be this endogenous ligand and that it has a crucial role in regulating insulin sensitivity via Tlr4 signaling in mice. *FetA* (officially known as *Ahsg*) knockdown in mice with insulin resistance caused by a high-fat diet (HFD) resulted in downregulation of Tlr4-mediated inflammatory signaling in adipose tissue, whereas selective administration of FetA induced inflammatory signaling and insulin resistance. FFA-induced proinflammatory cytokine expression in adipocytes occurred only in the presence of both FetA and Tlr4; removing either of them prevented FFA-induced insulin resistance. We further found that FetA, through its terminal galactoside moiety, directly binds the residues of Leu100–Gly123 and Thr493–Thr516 in Tlr4. FFAs did not produce insulin resistance in adipocytes with mutated Tlr4 or galactoside-cleaved FetA. Taken together, our results suggest that FetA fulfills the requirement of an endogenous ligand for TLR4 through which lipids induce insulin resistance. This may position FetA as a new therapeutic target for managing insulin resistance and type 2 diabetes.

Insulin resistance is one of the major outcomes of chronic inflammation fueled by FFAs[10–13]. There has been growing evidence over the last few years that FFA-induced production of proinflammatory cytokines from inflamed adipose tissue is mediated through TLR4, a pattern recognition receptor. FFA-mediated activation of the TLR4 and nuclear factor-κB (NF-κB) pathways has been increasingly recognized as a cause of insulin resistance[4–8]; however, in the absence of a direct association between FFAs and the TLR4-MD2 complex[8,9], how FFAs activate TLR4 signaling remains unresolved. This has created a crucial deficiency in the understanding of the regulation of the FFA-TLR4 signaling pathway. Identification of an endogenous ligand that allows FFA-TLR4 crosstalk is therefore crucial to our understanding of the mechanism by which FFAs induce insulin resistance.

FetA, a liver secretory glycoprotein, stimulates the production of inflammatory cytokines from adipocytes and macrophages and therefore acts as a biomarker of chronic inflammatory diseases[14–16]. We have demonstrated that FFAs cause FetA overexpression through NF-κB[17] and that elevation of FetA's circulatory level enhanced proinflammatory cytokine production from adipocytes[17,18]. Notably, *FetA*- or *Tlr4*-knockout mice are protected from HFD-induced insulin resistance[4,19–21] and it has also been reported that FetA acts as a major carrier protein of FFAs in the circulation[22]. On the basis of these reports, we hypothesized that FetA may present FFAs to TLR4 by its actions as an endogenous ligand for this receptor.

To examine our hypothesis, we determined FetA concentration in serum, as well as *TLR4, IL-6* and *TNF-α* expression and NF-κB activation in adipocytes, isolated from obese diabetic human subjects, HFD-induced insulin resistant mice and dyslipidemic *db/db* mice. We found that all of these parameters were significantly elevated in these conditions in comparison with nonobese nondiabetic human subjects, standard diet (SD)-fed BALB/c mice and wild-type BL/6 mice, respectively (**Fig. 1a** and **Supplementary Fig. 1a**). This suggests an association between lipid, FetA concentration and TLR4 expression and activation in states of insulin resistance.

As $FetA^{-/-}$ and $Tlr4^{-/-}$ mice are protected from lipid-induced insulin resistance[4,19–21], we thought that using them to examine FetA-TLR4 interdependence in producing insulin resistance might not be useful. We therefore prepared diet-induced insulin-resistant mice and then used vivo-morpholino (VMO)-based gene knockdown of *FetA* or *Tlr4* ($FetA^{KD}$ or $Tlr4^{KD}$ mice; we verified knockdown efficiency by real-time quantitative PCR (qPCR), but knockdown did not significantly alter body and adipose tissue weight) (**Supplementary Fig. 1b**,**c**), as this would be an ideal model to understand the FetA-Tlr4 association in implementing insulin resistance. $FetA^{KD}$ or $Tlr4^{KD}$ mice were protected from insulin resistance due to a HFD, as was evident from differences in blood glucose levels, [^{14}C]-2-deoxy-D-glucose ([^{14}C]-2DOG) uptake, responses to

[1]Cellular and Molecular Endocrinology Laboratory, Centre for Advanced Studies in Zoology, School of Life Science, Visva-Bharati (A Central University), Santiniketan, West Bengal, India. [2]Council of Scientific and Industrial Research (CSIR)–North-East Institute of Science and Technology (NEIST), Jorhat, India. [3]Immunology Group, International Centre for Genetic Engineering and Biotechnology, New Delhi, India. [4]Department of Endocrinology & Metabolism, Institute of Post-Graduate Medical Education & Research-Seth Sukhlal Karnani Memorial Hospital (IPGME&R-SSKM) Hospital, Kolkata, India. [5]Division of Surgical Gastroenterology, IPGME&R-SSKM Hospital, Kolkata, India. [6]Division of Cellular Endocrinology, National Institute of Immunology, New Delhi, India. [7]These authors contributed equally to this work. Correspondence should be addressed to S.B. (bhattacharyasa@gmail.com).

Received 1 March; accepted 31 May; published online 29 July 2012; doi:10.1038/nm.2851

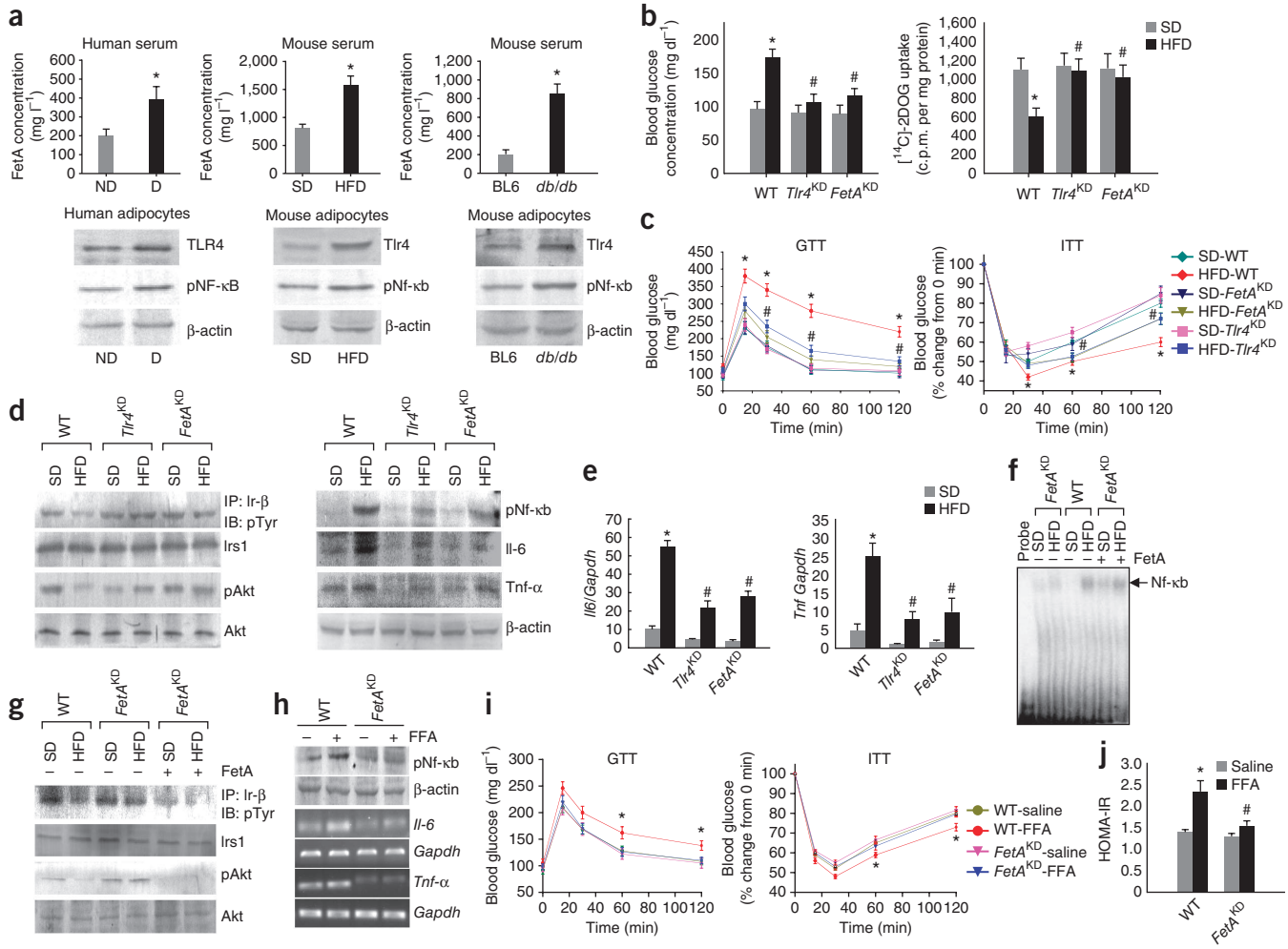

Figure 1 FetA effect on lipid-induced TLR4 activation in adipocytes. (**a**) ELISA of serum FetA (top) and western blot of TLR4 and pNF-κB level (bottom) in the adipose tissue of human subjects without diabetes (ND, $n = 12$) or with diabetes (D, $n = 10$); standard-diet (SD)- or HFD-fed mice ($n = 6$); and BL6 or *db/db* mice; ($n = 5$). $^{*}P < 0.01$ versus ND, SD or BL6. Parameters for insulin resistance was determined in SD- or HFD-fed WT or *Tlr4*^{KD} or *FetA*^{KD} mice. (**b**) Blood glucose concentration (left) and [^{14}C]-2DOG uptake by skeletal muscle cells (right). (**c**) Glucose tolerance test (GTT, left) and insulin tolerance test (ITT, right) $^{*}P < 0.01$ versus SD-WT; $^{\#}P < 0.05$ versus HFD-WT. (**d**) Western blot showing phosphorylation status of insulin receptor β (Ir-β) and Akt (left) along with pNf-κb, Il-6 and Tnf-α abundance (right). IP; immunoprecipitation; IB; immunoblot. (**e**) Quantification of *Il-6* and *Tnf-α* mRNA expression in adipose tissue of the above-mentioned mice, $^{*}P < 0.001$ versus SD-WT; $^{\#}P < 0.01$ versus HFD-WT. (**f**,**g**) Electrophoretic mobility shift assay demonstrating Nf-κb binding to DNA (**f**) and western blot showing pIr-β and pAkt abundance (**g**) in the adipose tissue from SD-*FetA*^{KD} and HFD-*FetA*^{KD} mice in response to FetA. (**h**) Western blot of pNf-κb and RT-PCR of *Il-6* and *Tnf-α* in the adipose tissue of saline- or FFA-infused WT and *FetA*^{KD} mice ($n = 5$). β-actin or Irs1 or Akt or *Gapdh* was used as loading control. (**i**) GTT and ITT in saline- or FFA-infused WT and *FetA*^{KD} mice ($n = 5$), $^{*}P < 0.05$ versus *FetA*^{KD}-FFA. (**j**) HOMA-IR in saline- or FFA-infused WT and *FetA*^{KD} mice ($n = 5$). $^{*}P < 0.05$ versus WT-saline; $^{\#}P < 0.05$ versus WT-FFA. Data represent means ± s.e.m.

a glucose tolerance test (GTT) and an insulin tolerance test (ITT), homeostasis model assessment–insulin resistance (HOMA-IR) scores and phosphorylation of the insulin-signaling molecules insulin receptor-β (Ir-β) and Akt (**Fig. 1b–d** and **Supplementary Fig. 1d**), suggesting that both FetA and Tlr4 are necessary for lipid-mediated insulin resistance in our mouse model. This was further indicated by the reduced Nf-κb activity along with the marked reduction of interleukin-6 (*Il-6*) and tumor necrosis factor-α (*Tnf-α*) mRNA expression in adipocytes from *FetA*^{KD} and *Tlr4*^{KD} mice as compared to wild-type mice under the same dietary regimen. (**Fig. 1e**).

The involvement of TLR4 in lipid-induced insulin resistance has been shown previously[4–7], therefore it was expected, but we were intrigued by the similar trend of the results in *FetA*^{KD} mice. Thus, to validate our findings further, we introduced FetA, free of endotoxin (a TLR4 ligand expressed by bacteria and hence a common contaminant in recombinant proteins isolated from bacterial expression systems) (**Supplementary Fig. 1e–h**) to *FetA*^{KD} mice and found this manipulation resulted in lipid-induced insulin resistance (**Fig. 1f,g** and **Supplementary Fig. 1d**).

As the liver is a major source of FetA, we partially hepatectomized rats to lower the serum levels of FetA as an alternative means to genetically knocking down the expression of the protein. We observed a significant decrease in serum FetA levels along with a reduction in pNf-κb, Il-6 and Tnf-α in partially hepatectomized HFD rats as compared to control HFD rats (**Supplementary Fig. 1i**).

Adipose tissue from lipid-infused *FetA*^{KD} mice did not show Tlr4 activation, whereas it was apparent in wild-type (WT) mice (**Fig. 1h**). Glucose and insulin tolerances were decreased, and

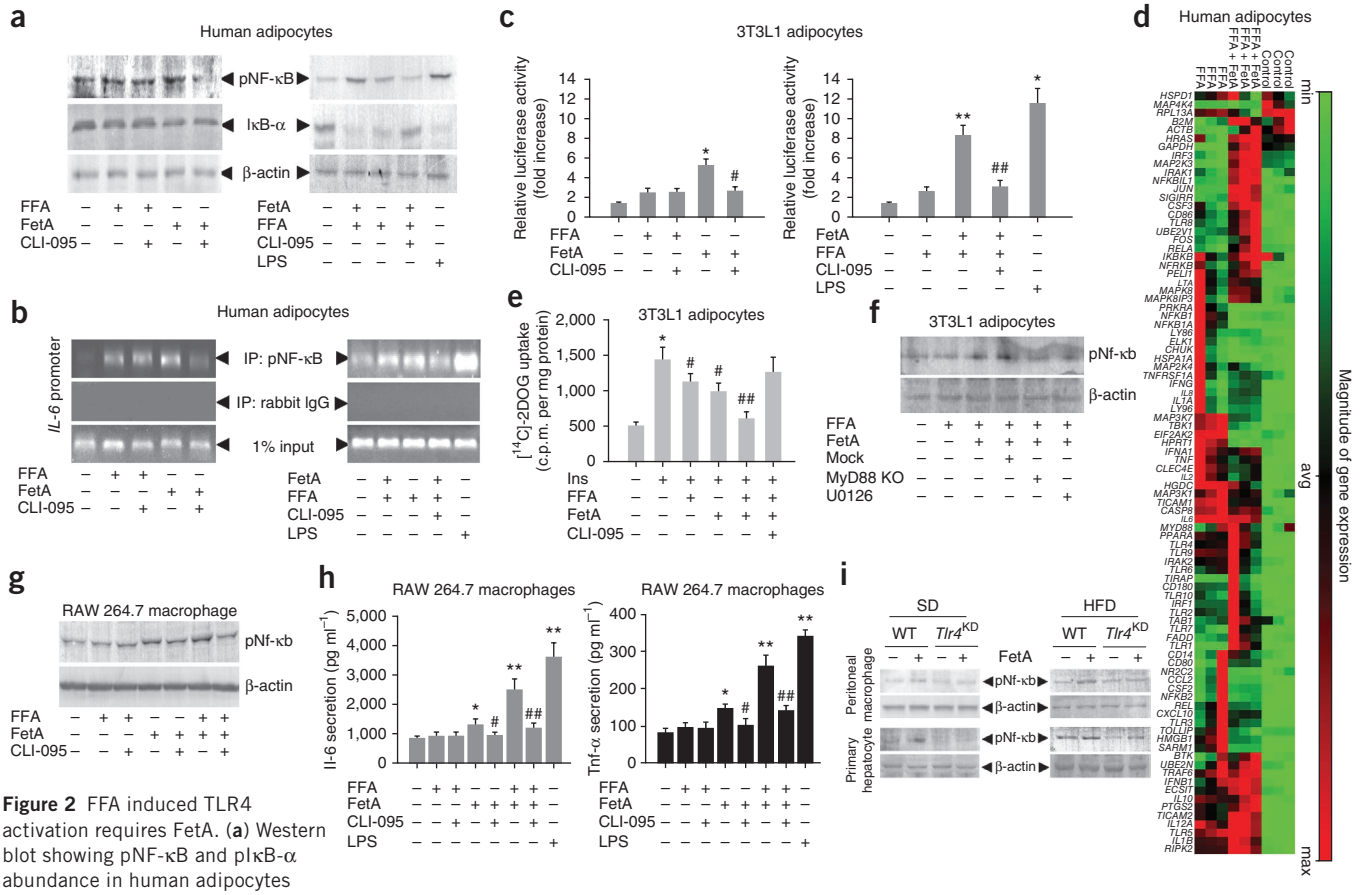

Figure 2 FFA induced TLR4 activation requires FetA. (**a**) Western blot showing pNF-κB and pIκB-α abundance in human adipocytes incubated with FFA or FetA (left) or FFA or FFA + FetA (right) in the absence or presence of CLI-095. Lipopolysaccharide (LPS) was used as positive control. (**b**,**c**) ChIP assay showing Nf-κb binding to an *Il-6* promoter in human adipocytes (**b**) and the determination of relative luciferase activity in 3T3L1 adipocytes (**c**) after the incubation of FFA or FetA (left panel) or FFA or FFA + FetA (right panel) in the absence or presence of CLI-095. $^{*}P < 0.01$, $^{**}P < 0.001$ versus Control (–); $^{\#}P < 0.01$ versus FetA, $^{\#\#}P < 0.001$ versus FFA + FetA. (**d**) PCR array showing the gene expression of TLR4 pathway components in human adipocytes treated without (control) or with FFA or FFA + FetA. (**e**) [^{14}C]-2DOG uptake by 3T3L1 adipocytes in response to the indicated conditions. $^{*}P < 0.001$ versus Control (–); $^{\#}P < 0.05$ versus insulin (Ins); $^{\#\#}P < 0.01$ versus Ins. (**f**) Western blot of pNf-κb level in MyD88-knockout (KO) or U0126-incubated 3T3L1 adipocytes. (**g**) Western blots showing pNf-κb level in macrophage cells incubated under the indicated conditions. (**h**) ELISA showing Il-6 (left) and Tnf-α (right) secretion from the macrophages. $^{*}P < 0.05$, $^{**}P < 0.001$ versus Control (–); $^{\#}P < 0.05$ versus FetA, $^{\#\#}P < 0.001$ versus FFA + FetA. (**i**) Western blots showing pNf-κb level in peritoneal macrophages and primary hepatocytes obtained from SD- or HFD-fed WT and *Tlr4*^{KD} mice without or with FetA incubation. Values are means ± s.e.m.

insulin resistance was increased after palmitate infusion in WT mice, whereas in *FetA*^{KD} mice these parameters were unchanged (**Fig. 1i**,**j** and **Supplementary Fig. 1j**).

These results implicate three important possibilities regarding the involvement of FetA and Tlr4 in lipid-induced insulin resistance: (i) the decrease in Nf-κb phosphorylation in the absence of FetA may be due to impaired Tlr4 signaling, (ii) insulin resistance due to lipotoxicity requires the presence of both Tlr4 and FetA, and (iii) a physical association between FFAs, FetA and Tlr4 is likely to be linked to insulin resistance.

To address the first possibility, we investigated whether FFA-induced Tlr4 signaling requires FetA. Palmitate (a FFA) had maximum binding to FetA and produced the highest inflammatory response in 3T3L1 mouse adipocytes as compared to other FFAs (**Supplementary Fig. 2a**,**b**). We therefore incubated human adipocytes or 3T3L1 cells with palmitate or FetA or both of them in the absence or presence of CLI-095, a TLR4 signaling inhibitor, followed by the determination of NF-κB activity through western blotting, chromatin immunoprecipitation (ChIP) and reporter assays. FFA-induced activation of NF-κB and elevated expression of the cytokines *IL-6* and *TNF-α* occurred only in the presence of FetA, whereas CLI-095 incubation or silencing of Tlr4 expression by siRNA prevented this activation and cytokine expression (**Fig. 2a**–**c** and **Supplementary Fig. 2c**,**d**).

These results were notable given previous reports suggesting that FFAs activate the Tlr4 signaling pathway in 3T3L1 adipocytes[2,4,6,23,24]. One possibility for this disparity could be the high FetA concentration in FBS[25]. As commercially available FBS contains ~20 mg ml^{-1} FetA, conventionally used culture media (with 10% FBS) have a substantial amount of FetA, which might allow exogenously added FFAs to induce Tlr4 activation. We therefore used serum-free medium in our experiments. FFAs alone had a marginal stimulatory effect that seemed to be independent of Tlr4 because addition of CLI-095 to the medium did not alter the response to exogenous FFAs (**Fig. 2a**–**c**). That FFA can induce inflammatory signaling pathways independent of Tlr4 influence has also been shown by others[26,27]. In contrast, stimulation of Nf-κb activation by FetA was inhibited by CLI-095, indicating that FetA's effect is mediated through Tlr4 (**Fig. 2a**–**c**).

We made similar observations when we incubated macrophages and adipocytes obtained from *Tlr4*$^{-/-}$ mice (Tlr4 knockout was verified by RT-PCR, **Supplementary Fig. 2e**) with FetA and saw that FetA did

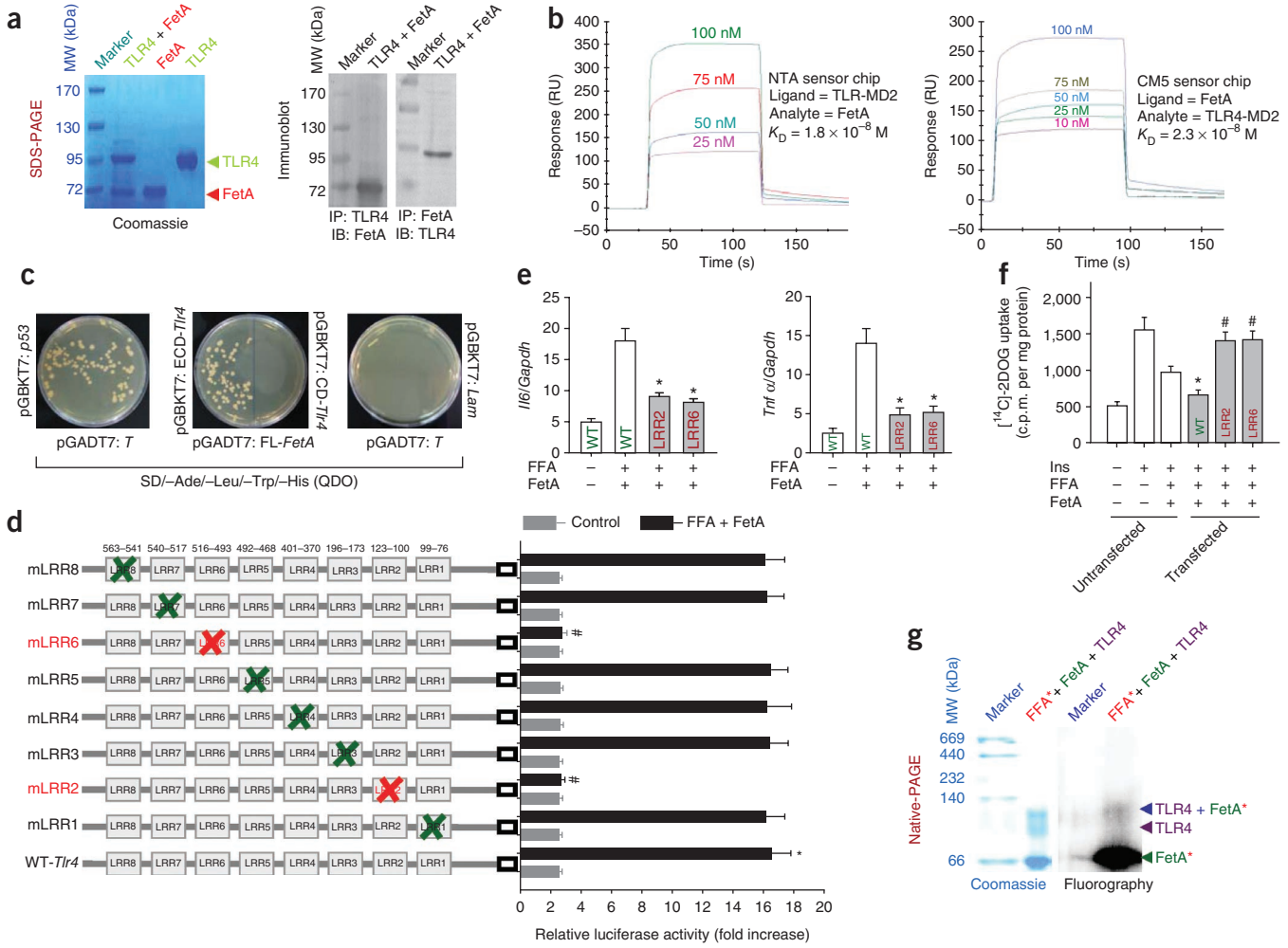

Figure 3 FetA-TLR4 interaction induces proinflammatory cytokine expression and insulin resistance in adipocytes. (**a**) SDS-PAGE (left) and western blot (right) of coimmunoprecipitation study demonstrating FetA binding to TLR4. (**b**) SPR study showing representative sensorgrams obtained from flowing of the indicated concentrations of FetA (left) or TLR4-MD2 (right) over the TLR4-MD2 immobilized NTA sensor chip or FetA immobilized CM5 sensor chip, respectively. Sensorgrams are represented as response units (RU) at specified time (s). (**c**) Y2H showing FetA binding with the extracellular domain (ECD) of *Tlr4* as indicated by the growth colonies in growth-limiting plates. pGADT7-*t* and pGBKT7-*p53* plasmids and pGADT7-*t* and pGBKT7-*Lam* plasmids were used as positive and negative controls, respectively. (**d**) Schematic structure showing the eight predicted LRR regions in the ECD of Tlr4. These were individually mutated by site-directed mutagenesis (left), and transfected 3T3L1 adipocytes were examined for *Nf-κb* luciferase activity (right). $^*P < 0.001$ versus control (–); $^{\#}P < 0.001$ versus WT *Tlr4*. (**e**) Quantification of *Il-6* and *Tnf-α* mRNA expression. $^*P < 0.01$ versus WT *Tlr4*. (**f**) [^{14}C]-2DOG uptake in WT, LRR2-mutated and LRR6-mutated *Tlr4*–transfected 3T3L1 adipocytes. $^*P < 0.05$ versus WT *Tlr4* untransfected; $^{\#}P < 0.01$ versus WT *Tlr4* transfected. (**g**) Representative gels of native-PAGE and its fluorography showing formation of a ternary complex between FFA, FetA and TLR4 (asterisks represent [^{3}H]-palmitate and its association with FetA). Data represent means ± s.e.m.

not activate the Tlr4 pathway, thus indicating the requirement of Tlr4 for FetA's effect on Nf-κb activation (**Supplementary Fig. 2f**). We also evaluated FFA plus FetA (FFA+FetA) induction of TLR4 signaling by PCR array and found that gene expression of various proinflammatory cytokines in human adipocytes belonging to the TLR4 pathway were greatly upregulated, whereas FFA alone produced a marginal effect (**Fig. 2d**). This was also reflected in the insulin sensitivity assay, wherein FFA+FetA showed a significantly greater inhibitory effect on insulin-stimulated [^{14}C]-2DOG uptake by 3T3L1 adipocytes as compared to FFA or FetA alone (**Fig. 2e**).

Because myeloid differentiation primary response gene 88 (MyD88) and mitogen-activated protein kinase kinase (MEK) are downstream of the TLR4 signaling pathway[28,29], failure of Nf-κb activation in MyD88-knockout 3T3L1 adipocyte cells incubated with FFA+FetA or in cells preincubated with the MEK inhibitor U0126 (**Fig. 2f**) suggest that FFA+FetA acts through the Tlr4 pathway. We found that FFA+FetA experiments with macrophages also had similar results; FFA augmentation of Tlr4 activation was dependent on FetA (**Fig. 2g,h**), as observed with adipocytes, indicating a link between insulin resistance and innate immunity with FFAs as reported earlier[4]. We examined this further in primary cell cultures of macrophage and hepatocytes obtained from standard diet–fed *Tlr4*^{KD} mice, in which FetA alone failed to induce Nf-κb activation but did so in standard diet–fed WT mice (**Fig. 2i**). We obtained similar results with HFD-fed insulin-resistant mice (**Fig. 2i**), suggesting that Tlr4 is necessary to produce the FFA+FetA effect on Nf-κb activation.

From these results it would seem evident that FetA is required for FFA-TLR4 signaling. However, we along with others have observed

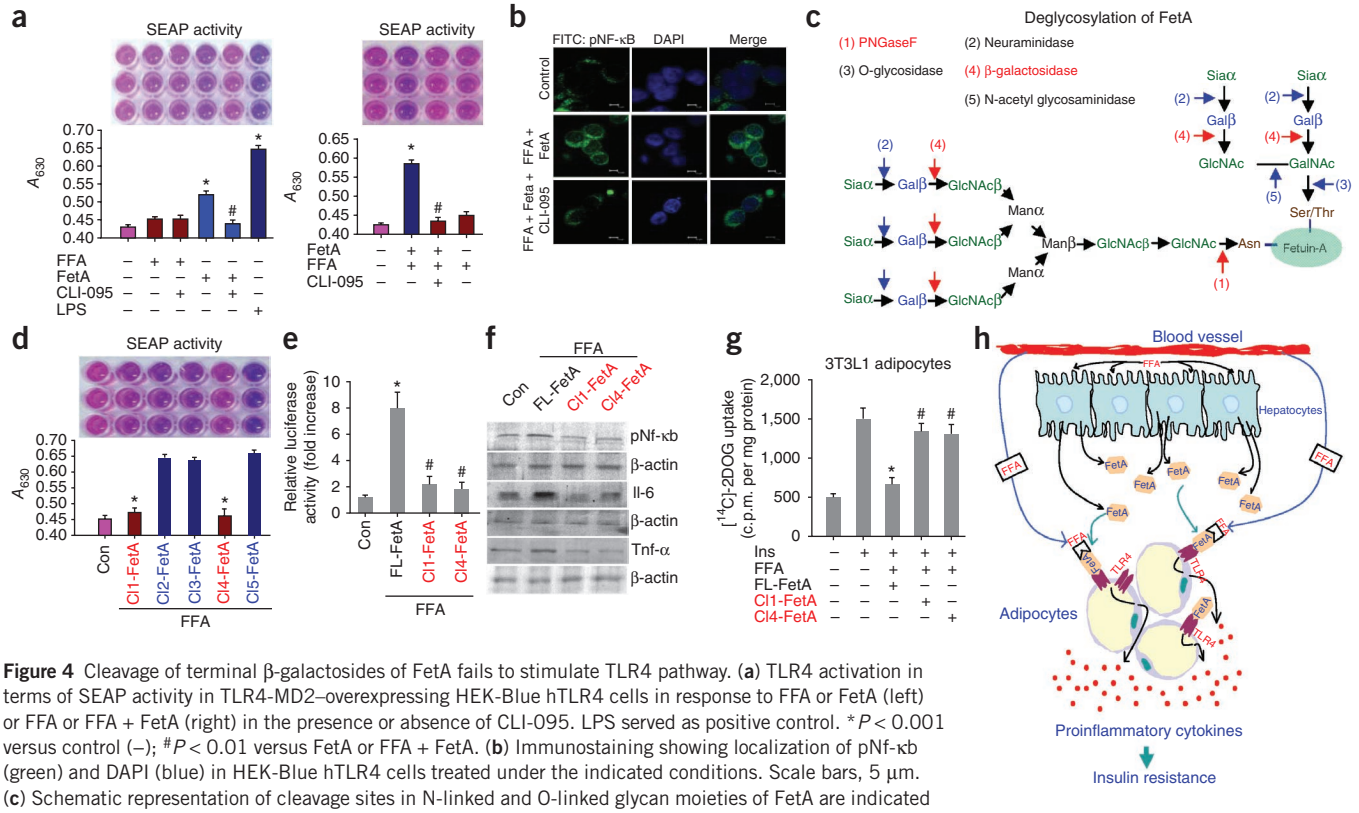

Figure 4 Cleavage of terminal β-galactosides of FetA fails to stimulate TLR4 pathway. (**a**) TLR4 activation in terms of SEAP activity in TLR4-MD2–overexpressing HEK-Blue hTLR4 cells in response to FFA or FetA (left) or FFA or FFA + FetA (right) in the presence or absence of CLI-095. LPS served as positive control. $^{*}P < 0.001$ versus control (–); $^{\#}P < 0.01$ versus FetA or FFA + FetA. (**b**) Immunostaining showing localization of pNf-κb (green) and DAPI (blue) in HEK-Blue hTLR4 cells treated under the indicated conditions. Scale bars, 5 μm. (**c**) Schematic representation of cleavage sites in N-linked and O-linked glycan moieties of FetA are indicated by red and blue arrows. Sia, sialic acid; Gal, galactose; Man, mannose; GlcNAc, N-acetylglucosamine; GalNAc, N-acetylgalactosamine; Asn, Asparagine, Ser/Thr: Serine/Threonine. (**d**) Inhibition of SEAP activity in response to cleaved FetAs (Cl1 and Cl4) by PNGaseF and β-galactosidase enzymes. $^{*}P < 0.001$ versus Cl2, Cl3 and Cl5. (**e**) Inhibition of Nf-κb reporter activity in 3T3L1 adipocytes treated with FFA plus Cl1 or Cl4 FetA. $^{*}P < 0.001$ versus Control (–); $^{\#}P < 0.01$ versus full-length FetA (FL-FetA). (**f**,**g**) Western blot showing pNf-κb, Il-6 and Tnf-α abundance in 3T3L1 adipocytes (**f**) and [^{14}C]-2DOG uptake by 3T3L1 adipocytes (**g**) incubated with FL or cleaved FetAs (Cl1 and Cl4). $^{*}P < 0.01$ versus Ins; $^{\#}P < 0.01$ versus FL-FetA. Values are means ± s.e.m. (**h**) Proposed model highlighting the requirement of FetA in lipid-induced TLR4 activation that leads to insulin resistance. Error bars represent mean ± s.e.m.

that FFAs have no direct association with TLR4 (refs. 8,9), whereas they bind FetA appreciably[22] (**Supplementary Fig. 3a**). We found further evidence of these facts in a lipid-protein overlay assay where FFAs bound FetA but not TLR4 (**Supplementary Fig. 3b**). Hence, it is possible that FetA acts as an intermediary between FFA and TLR4. Indeed, coimmunoprecipitation revealed the existence of a complex between FetA and TLR4 (**Fig. 3a** and **Supplementary Fig. 3c**).

To study the nature of this complex and to probe the possibility of a physical interaction between FetA and TLR4 as proposed above, we performed surface plasmon resonance (SPR) in which varied concentrations of FetA were flowed over a histidine-tagged human TLR4-myeloid differentiation factor 2 (MD2) complex which was immobilized on a nitrilotriacetic acid (NTA) sensor chip. The resulting sensorgram showed concentration-dependent binding of FetA to TLR4, and the affinity of this binding was appreciably high, as indicated by its K_D value (1.8×10^{-8} M). Reversing the situation, wherein FetA remained immobilized on the carboxymethylated dextran (CM5) chip and TLR4 was used as analyte, produced a similar binding affinity ($K_D = 2.3 \times 10^{-8}$ M) (**Fig. 3b**). The inability of high mobility group A1 (HMGA1) to interact with TLR4 indicates the specificity of this interaction (**Supplementary Fig. 3d**).

To examine whether such a complex between FetA and TLR4 is operative in an intracellular system, we performed a yeast two-hybrid (Y2H) assay using pGBKT7 fused with DNA encoding the extracellular domain or cytosolic domain of Tlr4. These plasmids were separately transfected into the Y2H Gold strain of yeast, followed by mating with the Y187 strain containing full-length *FetA* inserted into pGADT7. FetA interacted with the extracellular domain of Tlr4, as interaction-dependent growth of colonies was observed in SD/–Ade/–His/–Leu/–Trp (quadruple dropout, QDO) plates, whereas colony growth did not occur after mating with yeast expressing the plasmid encoding the cytoplasmic domain of Tlr4 (**Fig. 3c**).

We then searched the probable sites of the TLR4 extracellular domain to which FetA binds. We presumed it could be the region of leucine-rich repeats (LRR), as those have been previously found to be involved in protein-protein interactions[30]. To analyze FetA recognition of specific LRR sites, we mutated different LRRs in *Tlr4*. Deletion mutation of LRR2 (Leu100–Gly123) or LRR6 (Thr493–Thr516) in the extracellular domain of Tlr4 impeded its interaction with FFA+FetA, as indicated by diminished Nf-κb luciferase activity (**Fig. 3d**) and cytokine expression (**Fig. 3e**) in differentiated adipocytes and by α-galactosidase activity in Y2H studies (**Supplementary Fig. 3e**). Deletion mutations at these sites not only restored but also augmented insulin sensitivity (**Fig. 3f**), possibly because of the dominant-negative nature of the mutations (**Fig. 3d**). Mutational studies suggest that these two LRRs of Tlr4 are the crucial sites where FetA binds and permits FFAs to exert their deleterious effect on insulin activity. Hence, it is possible that FFAs, FetA and TLR4 all form one complex. To examine this, we incubated [^{3}H]-palmitate with FetA followed by human TLR4 incubation. Both Coomassie staining and flurography of the native-PAGE gel revealed a ternary complex between the three of them (**Fig. 3g**).

To determine the biological relevance of FetA-TLR4 interactions in FFA-induced insulin resistance, we used genetically engineered HEK-Blue hTLR4 cells, which contain a TLR4–NF-κB–secreted embryonic alkaline phosphatase (SEAP) reporter system to detect TLR4–NF-κB activation. Incubation of FFAs in the presence of FetA enhanced SEAP activity, which was inhibited by CLI-095 (**Fig. 4a**), and this was dose and time dependent (**Supplementary Fig. 4a–c**), indicating that FFA+FetA operates through the TLR4 pathway. Immunofluorescence study further supported the notion that both FetA and TLR4 are required to transduce FFA signals, because FFA+FetA-stimulated nuclear translocation of NF-κB was abrogated by CLI-095 (**Fig. 4b**).

We identified the sequence of TLR4 where FetA binds; however, which part of FetA recognizes the TLR4 sequence remained unanswered. As terminal carbohydrate moieties of glycoproteins, such as sialic acid, galactose and fucose, underpin cell adhesion, receptor recognition and host-pathogen interactions[31], we presumed that the glycan moieties of FetA bind TLR4, especially as Gram-negative bacteria trigger TLR4 signaling through the glycan residues of lipopolysaccharide[32–34]. To investigate this possibility, we used various enzymes to cleave specific glycosidic and amide bonds in FetA, as indicated (**Fig. 4c**). Truncated FetA and FetA's glycan part, obtained by enzymatic cleavage, were separately added to HEK-Blue hTLR4 cells. β-galactosidase– or PNGaseF-cleaved FetA was unable to stimulate SEAP activity (**Fig. 4d** and **Supplementary Fig. 4d**). Given that these results coincided with lower *Nf-κb* promoter activity and a concomitant reduction of proinflammatory cytokines expression (**Fig. 4e**,**f** and **Supplementary Fig. 4e**), the terminal β-galactoside moiety of FetA seems crucial for recognizing TLR4. We show that β-galactosidase–cleaved FetA did not produce FFA-induced insulin resistance in adipocytes (**Fig. 4g**).

The pathway in which FFA–FetA–induced TLR4 activation causes insulin resistance is presented in a schematic diagram (**Fig. 4h**). The influence of dietary lipids on the activation of the TLR4–NF-κB pathway to produce proinflammatory cytokines, resulting in insulin resistance, has long been known. The amount of fat in HFD could be a factor in TLR4-mediated insulin resistance; 45% fat in HFD has been shown to be insufficient to produce such response[35], whereas 55–60% fat in HFD effected insulin resistance through TLR4 (refs. 4,20,36). We have used HFD with 65% fat, which clearly induced insulin resistance. However, the molecular pathways that underlie a FFA-TLR4 interaction continue to elude investigators. FetA is a major carrier protein of FFAs in the circulation[22], and in the absence of FFAs directly binding to TLR4[8,9], we envisioned an endogenous presenter of FFAs to TLR4. We have shown here that FetA serves this purpose, as it physically interacts with both FFAs and TLR4. Moreover, our work has indicated a key role of FetA in FFA-induced TLR4 activation in adipocytes and thus in insulin resistance. These findings further suggest that FetA represents a potentially new target for developing therapeutics in the management of lipid-induced insulin resistance and type 2 diabetes.

METHODS

Methods and any associated references are available in the online version of the paper.

Note: Supplementary information is available in the online version of the paper.

ACKNOWLEDGMENTS

This research was financially supported by a grant from the CSIR and Department of Science and Technology, Ministry of Science and Technology, New Delhi. We thank the National Centre for Cell Science, Pune, India, for providing the 3T3L1 cell line; A. Bandyopadhyay and S. Roy of the Indian Institute of Chemical Biology, Kolkata for their help in the confocal and SPR work, respectively. D.P. is thankful to CSIR, New Delhi, for the award of Senior Research Fellowship. S.D. thanks the University Grants Commission (UGC), New Delhi, for the award of a UGC-Dr. D.S. Kothari postdoctoral fellowship and CSIR-NEIST for a Quick Hire Fellowship. S.B. thanks the Indian National Science Academy for his Senior Scientist position. G.D. gratefully acknowledges the gift of *Tlr4*$^{-/-}$ mice from R. Medzhitov, Yale School of Medicine. The authors appreciate the use of facilities as extended to us by the head of the Department of Zoology, Visva-Bharati University, Santiniketan; the director of IICB, director of IPGME&R-SSKM Hospital, Kolkata; the director of the National Institute of Immunology, director of ICGEB, New Delhi and the director of NEIST, Jorhat, India.

AUTHOR CONTRIBUTIONS

D.P. and S.D. designed and performed all the experiments, analyzed the data and wrote the manuscript; R.K. generated VMO–based *FetA* and *Tlr4* knockdown mice; G.D. performed lipid infusion study in WT and *FetA*^{KD} mice; S.R. provided nondiabetic and diabetic human blood and fat tissue; S.S.M. provided blood and tissue samples from WT and *db*/*db* mice; S. Maitra, G.D., S. Mukhopadhyay and S.S.M. wrote the manuscript; S.B. designed and supervised this study, analyzed the data and wrote the manuscript.

COMPETING FINANCIAL INTERESTS

The authors declare no competing financial interests.

Published online at http://www.nature.com/doifinder/10.1038/nm.2851.
Reprints and permissions information is available online at http://www.nature.com/reprints/index.html.

1. Lee, J.Y., Sohn, K.H., Rhee, S.H. & Hwang, D. Saturated fatty acids, but not unsaturated fatty acids, induce the expression of cyclooygenase-2 mediated through Toll-like receptor 4. *J. Biol. Chem.* **276**, 16683–16689 (2001).
2. Suganami, T. *et al.* Role of the Toll-like receptor 4/NF-κB pathway in saturated fatty acid–induced inflammatory changes in the interaction between adipocytes and macrophages. *Arterioscler. Thromb. Vasc. Biol.* **27**, 84–91 (2007).
3. Nguyen, M.T.A. *et al.* A subpopulation of microphages infiltrates hypertrophic adipose tissue and is activate by free fatty acids via Toll-like receptors 2 and 4 and JNK-dependent pathways. *J. Biol. Chem.* **282**, 35279–35292 (2007).
4. Shi, H. *et al.* TLR4 links innate immunity and fatty acid-induced insulin resistance. *J. Clin. Invest.* **116**, 3015–3025 (2006).
5. Kim, J.K. Fat uses a TOLL-road to connect inflammation and diabetes. *Cell Metab.* **4**, 417–419 (2006).
6. Fessler, M.B., Rudel, L.L. & Brown, J.M. Toll-like receptor signaling links dietary fatty acids to the metabolic syndrome. *Curr. Opin. Lipidol.* **20**, 379–385 (2009).
7. Kim, F. *et al.* Toll-like receptor-4 mediates vascular inflammation and insulin resistance in diet-induced obesity. *Circ. Res.* **100**, 1589–1596 (2007).
8. Schaeffler, A. *et al.* Fatty acid–induced induction of Toll-like receptor-4/nuclear factor-κB pathway in adipocytes links nutritional signalling with innate immunity. *Immunology* **126**, 233–245 (2009).
9. Erridge, C. & Samani, N.J. Saturated fatty acids do not directly stimulate Toll-like receptor signaling. *Arterioscler. Thromb. Vasc. Biol.* **29**, 1944–1949 (2009).
10. Xu, H. *et al.* Chronic inflammation in fat plays a crucial role in the development of obesity-related insulin resistance. *J. Clin. Invest.* **112**, 1821–1830 (2003).
11. Hotamisligil, G.S., Arner, P., Caro, J.F., Atkinson, R.L. & Spiegelman, B.M. Increased adipose tissue expression of tumor necrosis factor-α in human obesity and insulin resistance. *J. Clin. Invest.* **95**, 2409–2415 (1995).
12. de Luca, C. & Olefsky, J.M. Stressed out about obesity and insulin resistance. *Nat. Med.* **12**, 41–42 (2006).
13. Qatanani, M. & Lazar, M.A. Mechanisms of obesity-associated insulin resistance: many choices on the menu. *Genes Dev.* **21**, 1443–1455 (2007).
14. Mori, K. *et al.* Association of serum fetuin-A with insulin resistance in type 2 diabetic and nondiabetic subjects. *Diabetes Care* **29**, 468 (2006).
15. Stefan, N. *et al.* Plasma fetuin-A levels and the risk of type 2 diabetes. *Diabetes* **57**, 2762–2767 (2008).
16. Ix, J.H. & Sharma, K. Mechanisms linking obesity, chronic kidney disease, and fatty liver disease: the roles of fetuin-A, adiponectin, and AMPK. *J. Am. Soc. Nephrol.* **21**, 406–412 (2010).
17. Dasgupta, S. *et al.* NF-κB mediates lipid-induced fetuin-A expression in hepatocytes that impairs adipocyte function effecting insulin resistance. *Biochem. J.* **429**, 451–462 (2010).
18. Hennige, A.M. *et al.* Fetuin-A induces cytokine expression and suppresses adiponectin production. *PLoS ONE* **3**, e1765 (2008).
19. Mathews, S.T. *et al.* Improved insulin sensitivity and resistance to weight gain in mice null for the *Ahsg* gene. *Diabetes* **51**, 2450–2458 (2002).
20. Tsukumo, D.M.L. *et al.* Loss-of-function mutation in TLR4 prevents diet-induced obesity and insulin resistance. *Diabetes* **56**, 1986–1998 (2007).
21. Mathews, S.T. *et al.* Fetuin null mice are protected against obesity and insulin resistance associated with aging. *Biochem. Biophys. Res. Commun.* **350**, 437–443 (2006).

22. Cayatte, A.J., Kumbla, L. & Ravi Subbiah, M.T. Marked acceleration of exogenous fatty acid incorporation into cellular triglycerides by fetuin. *J. Biol. Chem.* **265**, 5883–5888 (1990).
23. Jiao, P. *et al.* Obesity-related upregulation of monocyte chemotactic factors in adipocytes involvement of nuclear factor-κB and c-Jun NH2–terminal kinase pathways. *Diabetes* **58**, 104–115 (2009).
24. Zu, L. *et al.* Bacterial endotoxin stimulates adipose lipolysis via Toll-like receptor 4 and extracellular signal-regulated kinase pathway. *J. Biol. Chem.* **284**, 5915–5926 (2009).
25. Mellgren, R.L. & Huang, X. Fetuin A stabilizes m-calpain and facilitates plasma membrane repair. *J. Biol. Chem.* **282**, 35868–35877 (2007).
26. Davis, J.E., Gabler, N.K., Daniel, J.W. & Spurlock, M.E. Tlr-4 deficiency selectively protects against obesity induced by diets high in saturated fat. *Obesity (Silver Spring)* **16**, 1248–1255 (2008).
27. Schwartz, E.A. *et al.* Nutrient modification of the innate immune response: a novel mechanism by which saturated fatty acids greatly amplify monocyte inflammation. *Arterioscler. Thromb. Vasc. Biol.* **30**, 802–808 (2010).
28. Barton, G.M. & Medzhitov, R. Toll-like receptor signaling pathways. *Science* **300**, 1524–1525 (2003).
29. Kawai, T. & Akira, S. TLR signaling. *Cell Death Differ.* **13**, 816–825 (2006).
30. Medzhitov, R., Preston-Hurlburt, P. & Janeway, C.A.J. A human homologue of the *Drosophila* Toll protein signals activation of adaptive immunity. *Nature* **388**, 394–397 (1997).
31. Paulson, J.C. & Colley, J.C.J. Glycosyltransferases. Structure, localization, and control of cell type-specific glycosylation. *J. Biol. Chem.* **264**, 17615–17618 (1989).
32. Park, B.S. *et al.* The structural basis of lipopolysaccharide recognition by the TLR4–MD-2 complex. *Nature* **458**, 1191–1195 (2009).
33. Barata, T.S., Teo, I., Brocchini, S., Zloh, M. & Shaunak, S. Partially glycosylated dendrimers block MD-2 and prevent TLR4–MD-2–LPS complex mediated cytokine responses. *PLoS Comput. Biol.* **7**, e1002095 (2011).
34. Ohto, U., Fukase, K., Miyake, K. & Satow, Y. Crystal structures of human MD-2 and its complex with antiendotoxic lipid IVa. *Science* **316**, 1632–1634 (2007).
35. Orr, J.S. *et al.* Toll-like receptor 4 deficiency promotes the alternative activation of adipose tissue macrophages. *Diabetes* published online, doi:10.2337/db11-1595 (29 June 2012).
36. Suganami, T. *et al.* Attenuation of obesity-induced adipose tissue inflammation in C3H/HeJ mice carrying a Toll-like receptor 4 mutation. *Biochem. Biophys. Res. Commun.* **354**, 45–49 (2017).

ONLINE METHODS

Animals and treatments. In the present study, we used control (C57BLKS/6J) and *db/db* (BKS.Cgm+/+Lepr(db)/J, stock no. 000642) female mice obtained from the Jackson Laboratory, using five mice in each treatment group. We made mice insulin resistant by providing HFD for 12 weeks. In percentage of total energy, the HFD consisted of 32.5% lard, 32.5% corn oil, 20% sucrose and 15% protein, whereas the SD contained 57.3% carbohydrate, 18.1% protein and 4.5% fat. The energy content of the standard diet was 15 kJ/g and the high-fat diet was 26 kJ g^{-1}. We procured Fetuin-A (5′-AAGACCAGG GACTTCATGGTTGCTC-3′; accession code: NM_013465.1), TLR4 (5′-AT GCAAGAGAGGCATCATCCTGGCA-3′; accession code: NM_019178.1) and their control VMOs from Gene Tools to generate $FetA^{KD}$ and $TLR4^{KD}$ mice. We treated 5- to 6-week-old female BALB/c mice with these VMOs. Twenty-five nmoles of VMO was delivered to tail vein through injection in each mouse for 5 consecutive days, one on each day. We also used $Tlr4^{-/-}$ mice, which were backcrossed ten generations on C57BL/6 background. WT littermates were used as controls. We determined GTT by estimating blood glucose concentration before and after oral gavages of 1g glucose per kg body weight at the indicated time points using Accu-Chek glucometer (Roche). ITT was assessed in a similar way by injecting 0.7 U insulin per kg body weight. We infused (1 µl h^{-1}) palmitate (600 mM) or saline for 8 d via a subcutaneous miniosmotic pump (Alzet, DURECT Corporation; Model 2001). Plasma insulin level was estimated by using Accu-Bind insulin ELISA kit (Monobind). Insulin function was evaluated by HOMA-IR and calculated as fasting insulin (µU per liter) × fasting glucose (mg dl^{-1})/405 (ref. 37). Mouse FetA (0.7 mg per g body weight) was administered in SD- and HFD-fed $FetA^{KD}$ mice by intravenous injection. Control mice received equal volumes of sterile PBS. All mouse experiments were performed following the guidelines prescribed by and with the approval of the Animal Ethics Committees of Visva-Bharati, International Centre of Genetic Engineering and Biotechnology and National Institute of Immunology.

Fetuin-A purification and deglycosylation. We purified FetA following the procedure of Li *et al.*[38] with slight modifications. We collected human and mouse serum and filtered through Amicon ultra-100K and 50K membrane filter devices (UFC510096 and UFC505096, Amicon Ultra Centrifugal Filters, Millipore) to obtain proteins between 50 kDa and 100 kDa. Samples were subjected to gel filtration chromatography using a HiPrep 26/60 Sephacryl S-100 high-resolution column. We loaded the FetA-enriched fraction on a column to remove serum albumin/IgGs (Pierce albumin/IgG removal kit, 89875). FetA-enriched elutant was then loaded onto a 5-ml Hitrap SP HP column, and bound FetA was collected by a linear NaCl gradient (50 mM sodium acetate). Purity of FetA was checked by SDS-PAGE (**Supplementary Fig. 1f**). We purchased a protein deglycosylation kit (Sigma, cat. no. EDEGLY) and used it for selective removal of glycan from FetA by PNGase F, α(2 3,6,8,9)-neuraminidase, O-glycosidase, β(1 4)-galactosidase and β-N-acetylglucosaminidase enzymes.

Removal of endotoxin contamination. We used EndoClear kit (EndoClear kit HIT307; Hycult Biotech) to remove endotoxin content in FFA (palmitate) and FetA preparations according to the manufacturer's instructions. Mouse FetA contained about 0.06 endotoxin units (EU) per ml and human FetA had around 0.08 EU ml^{-1} endotoxin. The endotoxin level of BSA-palmitate conjugate was 2.2 EU ml^{-1}. We passed all of the preparations separately through an EndoTrap Blue column to remove endotoxin contamination. Eluent was subsequently examined by Chromogenic Limulus Amebocyte Lysate (LAL) assay kit (HIT311, Hycult Biotech) to detect its endotoxin level. We repeated this removal procedure for several times until to the endotoxin concentration was very negligible, that is, 0.005–0.009 EU ml^{-1} (**Supplementary Fig. 1e**). We checked these levels of endotoxin by administering the preparations to 3T3L1 adipocytes and macrophages, which failed to produce a TLR4 response.

To further examine whether this negligible level of LPS could influence FetA- or FFA–FetA induced TLR4 activation, we conducted two experiments. First, Polymixin B (PMB) was incubated with adipocytes and macrophages in the presence of LPS, FFA, FetA or FFA+FetA followed by determination of TLR4 activity through NF-κB promoter reporter assay. PMB did not interfere with FetA- or FFA+FetA–induced TLR4 activation but blocked LPS-induced activation of TLR4 (**Supplementary Fig. 1f**). Second, we checked whether LPS binds FetA by incubating 60 EU per ml LPS (normal level of LPS in human serum[39]) with FetA and subjecting it to coimmunoprecipitation followed by western blotting with *Escherichia coli* LPS–specific mouse monoclonal antibody (clone number: 2D7/1; cat. no. ab35654, Abcam; dilution: 1:500 to show that LPS interacted with FetA (**Supplementary Fig. 1g**), which was also evident from TLR4 activation (**Supplementary Fig. 1h**).

Cell cultures and treatments. We isolated primary hepatocytes and peritoneal macrophages from WT and $Tlr4^{KD}$ mice and primary adipocytes and peritoneal macrophages from WT and $TLR4^{-/-}$ mice and incubated them with FetA for 4 h in DMEM/F12. 3T3L1 preadipocyte and RAW264.7 macrophage cells were cultured in DMEM containing penicillin (100 U ml^{-1}) and streptomycin (100 µg ml^{-1}) and supplemented with 10% FBS at 37 °C in humidified atmosphere with 5% CO_2. Two days after confluence, preadipocytes were stimulated to differentiate over 5 d in differentiation medium supplemented with 5 µg ml^{-1} insulin, 0.5 mmol per liter 3-isobutyl-1-methylxanthine and 1 µmol per liter dexamethasone. As conventionally used culture media usually contain 10% FBS that has substantial amount (~2 mg ml^{-1}) of FetA[25]. we washed differentiated 3T3L1 adipocytes thoroughly to remove FetA contamination, if any, and then carried out incubations/treatments with serum-free medium (SFM) without antibiotics. HEK-Blue hTLR4 cells (cat. no. hkb-htlr4) containing TLR4/NF-κB/SEAP [TLR4-NF-κB-SEAP] reporter was purchased from Invivogen, CA, USA, and was incubated at various concentrations (25, 50, 100 and 200 µg ml^{-1}) of FetA in the presence of 0.75 mM palmitate or different concentrations of palmitate (0.25, 0.50, 0.75 and 1.0 mM) with a fixed concentration of FetA (100 µg ml^{-1}). We performed time kinetics with 15, 30, 60, 120 and 240 min of incubation where both FetA (100 µg ml^{-1}) and palmitate (0.75 mM) were used at a fixed concentration. In case of cell incubations with inhibitors, CLI-095 (3 µM) or U0126 (10 µM) or polymixin B (100 µg ml^{-1}) were added 1 h before addition of FFA or FetA or both. In positive-control treatments, LPS (100 ng ml^{-1}) was used as TLR4 agonist for 4 h. We transfected MyD88 or TLR4 siRNA or wild-type TLR4 or mutated TLR4 vector into 3T3L1 adipocytes with Lipofectamine 2000 (Invitrogen, Carlsbad, CA, USA) following the manufacturer's protocol. Upon termination of incubations, cells were washed twice with ice-cold PBS and harvested with trypsin (0.25%)–EDTA (0.5 mM). NF-κB promoter reporter activity was assessed according to the manufacturer's instructions using Steady-Glo luciferase assay system (PromegaA) in cells transfected with pNF-κB-luc expression vector (PathDetect NF-κB *cis*-reporting system, Stratagene).

Human subjects. We obtained visceral adipose tissue from ten individuals with diabetes (four males and six females) and 12 individuals without diabetes (six males and six females), 54–69 years old, who were admitted to IPGME&R-SSKM Hospital and underwent abdominal surgery. With the due ethical committee clearance from the hospital, the Institutional Ethics Committee (IEC) approved the study and all the participants in this study gave written consent we also obtained blood and adipose tissue sample from the patients for the estimation of serum FetA level and inflammatory cytokines expression, respectively. Adipose tissue was rinsed with sterile 0.9% NaCl solution followed by washing with HBSS supplemented with 5.5 mM glucose. Adipose tissue was digested in HBSS buffer containing 5.5 mM glucose, 5% fatty acid-free BSA and 3.3 mg ml^{-1} type II collagenase for 30 min in a 37 °C water bath. The digestion mixture was passed through a tissue sieve and adipocytes were resuspended in SFM. Cells were plated in six-well culture plates and kept in a humidified 95% O_2/5% CO_2 atmosphere at 37 °C.

Reagents and antibodies. All tissue culture materials were obtained from Gibco-BRL/Life Technologies, Gaithersburg, USA. 3T3L1 preadipocyte cell differentiation was done by using Adipogenesis assay kit (cat. no. 10006908, Cayman Chemical Company). [U-^{14}C]-2- deoxyglucose (2-DOG) (cat. no. NEC042V250UC; specific activity 250–360 mCi per mmol) and [9,10-^{3}H(N)]-palmitate (cat. no. NET043005MC; specific activity 30–60 C per mmol) were obtained from GE Healthcare, and 5-ml Hitrap SP HP columns (cat. no. 17-1152-01), HiPrep 26/60 Sephacryl S-100 high resolution

doi:10.1038/nm.2851

columns (cat. no. 17-1165-01), HMW Native molecular weight marker (cat. no. 17-0445-01) and Amersham Hybond-C Extra (cat. no. RPN2020E) were obtained from GE Healthcare. [γ-^{32}P]ATP (cat. no. LCP 101; specific activity, 3800 Ci per mmol) was procured from Board of Radiation and Isotope Technology (BRIT). We purchased antibodies raised against pNF-κB p65 (Ser536 (cat. no. sc-101752)), IL-6 (sc-81026 and sc-1265), TNF-α (sc-1350), TLR4 (sc-10741) and FetA (sc-28924) from Santa Cruz Biotechnology. Anti-IκBα antibody (cat. no. 9242) was procured from Cell Signaling Technology and anti–*Escherichia coli* LPS antibody (cat. no. ab35654) was purchased from Abcam, Cambridge, MA, USA. Alkaline phosphatase–conjugated goat anti-rabbit antibodies, rabbit anti-goat antibodies, polymixin B sulfate and U0126 ethanolate were purchased from Sigma Chemical Co, Bethesda, MA, USA. PageRuler Prestained Protein Ladder (cat. no. SM0671) was obtained from Fermentas, Maryland, USA. Recombinant human TLR4 protein (cat. no. 3146/CF), human and mouse FetA DuoSet ELISA kit (cat. nos. DY1184 and DY1563), IL-6 and TNF-α Quantikine ELISA kit (cat. no. M6000B and cat. no. MTA00B) were purchased from R&D Systems, Minneapolis, MN, USA. All the primary antibodies used in western blotting at a dilution of 1:500 and secondary antibodies were used at 1:2,000 dilution. We have obtained purified human Fetuin-A and recombinant mouse FetA from Prospec Tany TechnoGene Ltd., East Brunswick, MN, USA (cat. no. PRO-418) and R&D Systems, Inc., Minneapolis, MN, USA (cat. no. 1563-PI-050), respectively. CLI-095 (cat. no. tlrl-cli95) and Ultrapure-Lipopolysaccharide (LPS) from *E. coli* 0111: B4 (cat. no. tlrl-pelps) were purchased from Invivogen, CA, USA. Human RT^2 Prolifer PCR array and all other RT^2-qPCR primers: *TLR4* (cat. no. PPH01795E (68 bp); *Tlr4* (cat. no. PPM04207F (93 bp); *FETA* (cat. no. PPH16956E (142 bp); *FetA* (cat. no. PPM32919B (170 bp), *IL6* (cat. no. PPH00560B (160 bp); *Il6* (cat. no. PM03015A (178 bp); *TNFα* (cat. no. PPH00341E (54 bp); *Tnfα* (cat. no. PM03113F (93 bp); *GAPDH* (cat. no. PPH00150E (175 bp); *Gapdh* (cat. no. PPM02946E (140 bp) were purchased from SA Biosciences, Frederick, MD, USA. We procured the Matchmaker Gold yeast two-hybrid system (cat. no. 630489) and QuickChange site-directed mutagenesis kit (cat. no. 200518) from Clontech Laboratories and Stratagene, respectively. Pierce albumin/IgG removal kit (cat. no. 89875) was obtained from Pierce. All other chemicals were procured from Sigma-Aldrich.

Western blots. We determined protein concentration of tissue extract or cell lysates or media following a previously described method[40]. We resolved 50 μg of protein sample on 10% SDS-PAGE and transferred it to PVDF membranes (Millipore) with the help of Semi-Dry Trans-Blot SD Cell (Bio-Rad Laboratories). The membranes were first incubated with primary antibody at 1:500 dilutions followed by goat anti-rabbit secondary antibody conjugated with alkaline phosphatase at 1:2,000 dilutions using SNAP ID apparatus (Millipore). The protein bands were detected by using 5-bromro 4-chloro 3-indolyl phosphate/nitroblue tetrazolium (BCIP/NBT).

Quantitative PCR. We extracted RNA from tissues or cells by using RNeasy Lipid Tissue Mini Kit (Qiagen) according to the manufacturer's instructions. RNA was treated with DNase I and reverse transcribed using Revert Aid first-strand cDNA synthesis kit (Fermentas). We used SYBR green–based real-time quantitative PCR reactions (Applied Biosystems) by using gene-specific primers obtained from SA Biosciences, Frederick, MD, USA. After the final extension, a melting curve analysis was performed to ensure the specificity of the products. *Gapdh* was simultaneously amplified in separate reactions and used for correcting the C_t value.

PCR array. We performed human Toll-like receptor signaling pathway PCR array (cat. no. PAHS-018A, SA Bioscience) by following the manufacturer's instructions. Briefly, first-strand cDNA was synthesized from 5 μg of RNA using the RT^2 First Strand Kit. A total volume of 25 μl of PCR reaction mixture, which included 12.5 μl of RT^2 Real-Time SYBR Green/ROX PCR master mix, 11.5 μl of nuclease-free water and 1 μl of template cDNA, was loaded in each well of the RT^2 Profiler PCR array. PCR amplification was performed in an ABI 7500 real-time PCR machine (Applied Biosystems). Data were imported into RT2 Proflier PCR array data analysis, version 3.5 to detect the alterations of gene expression. C_t values were normalized to housekeeping genes.

Eelectrophoretic mobility shift assay. We prepared nuclear extracts from cells under different incubations and subjected to electrophoretic mobility shift assay using oligonucleotide probes specific for the NF-κB binding site (5′-GCACCTGGGTTGGTCCCGAAGC-3′) as described previously[41]. The probes were end-labeled with $^{\gamma 32}$P-[ATP] using T4 polynucleotide kinase and incubated with 10 μg of nuclear extracts in a 20-μl reaction volume for 45 min on ice. Reaction mixture was resolved on a 5% (wt/vol) non-denaturing polyacrylamide gel and exposed to the phosphorimager screen, and the DNA/protein complexes were revealed on Storm phosphor-imager (GE Healthcare).

Chromatin immunoprecipitation assay. We performed ChIP by using ChIP assay kit (Upstate) according to our previous description[41] using 2 μg of anti–NF-κBp65 or anti-IgG antibodies. Primers used for amplification of the human *IL6* promoter sequence were 5′-CAGAGCACCTGGTTGGT-3′ (forward) and 5′-GCCCCAGAGCTGAGCAA-3′ (reverse). PCR products were run on ethidium bromide–stained 1.5% agarose gel, and the image was captured by the Bio-Rad gel documentation system using Image Lab software.

Coimmunoprecipitation. We conducted our coimmunoprecipitation study by following a method previously described[41]. Briefly, 200 μg of pure human FetA and Tlr4 proteins were incubated for 4 h followed by overnight incubation with FetA- or TLR4-specific antibody. The immunocomplex was precipitated with a 4-h incubation of protein-A agarose. Pelleted immunocomplex was washed thoroughly, boiled in 4× sample buffer, vortexed and then centrifuged at 15,000 r.p.m. for 10 min. Supernatant was isolated and run on 10% SDS-PAGE gel. This was followed by immunoblotting with either antibodies specific to TLR4 or FetA. Similarly, 200 μg of LPS was incubated with either FetA or TLR4 and subjected to immunoprecipitation by FetA- or TLR4-specific antibody followed by immunoblotting with LPS-specific antibody.

Lipid-protein overlay assay. We performed protein-lipid overlay assay by following an earlier description[42] with little modification. Briefly, the nitrocellulose membrane was spotted with increasing amounts of palmitate (1, 3 and 5 mM), and the membrane was blocked for 1 h in 2 ml of blocking buffer (3% fatty-acid-free BSA, 150 mM NaCl, 10 mM Tris pH 7.4) followed by incubation with 200 ng ml^{-1} of purified FetA or TLR4 protein overnight at 4 °C. The membrane was then incubated with a 1:500 dilution of anti-FetA or anti-TLR4 antibody for 1 h followed by 1 h incubation with 1:2,000 dilution of ALP-conjugated goat anti-rabbit secondary antibody, and FFA-bound protein was visualized by BCIP-NBT.

Immunofluorescence. We incubated paraformaldehyde-fixed cells overnight with anti–pNF-κBp65 polyclonal antibodies (dilution 1:100) followed by FITC-conjugated goat anti-rabbit secondary antibody (dilution 1:1,000) for 2 h. Cells were mounted in anti-fade mounting medium containing DAPI (Vector Laboratories, Inc.) for nuclear staining and followed by analysis with a laser scanning confocal microscope (Leica 224).

Surface plasmon resonance (BIAcore) study. We performed surface plasmon resonance experiments on a BIAcore 3000 instrument (BIAcore) using NTA and CM5 sensor chips according to manufacturer's instructions. Briefly, the NTA sensor chip was equilibrated with running buffer containing 10 mM HEPES (pH 7.5), 150 mM NaCl, 0.005% Surfactant P20, 50 mM EDTA) followed by priming the chip with 0.1 M $NiCl_2$. Pure His(C-terminal)-TLR4/MD2 complex was flowed over the Ni^{2+}-coated NTA sensor chip surface at a flow rate of 5 μl min^{-1}. The final amount of His-TLR4 protein covalently immobilized on the surface was 600 RU. Varied concentrations of FetA (25–100 nM) was sprayed over the immobilized TLR4 Ni^{2+}-primed NTA chip at a flow rate of 5 μl min^{-1} for 10 min. The CM5 sensor chip was used to direct immobilization of FetA by the amine-coupling method and followed by TLR4 protein run at various concentrations (10–100 nM) over it. In both cases, the sensorgram was corrected by subtracting the initial level of SPR signal before injection of the FetA or TLR4 and plotted as RU versus time. Binding kinetics were analyzed for one-to-one Langmuir binding model provided with BIA evaluation software. provided with BIA evaluation software.

Yeast two-hybrid assay. We conducted two-hybrid assays following the manufacturer's protocol of Matchmaker-Gold yeast two-hybrid assay kit. For this purpose we first amplified the extracellular domain or cytoplasmic domain of TLR4 and full-length FetA by PCR from adipocyte and hepatocyte cDNAs, respectively, followed by their cloning into pGBKT7 or pGADT7 vector flanked by EcoRI-BamHI. Constructs were in frame and sequenced to confirm the inserts. Primers used for this study are listed in **Supplementary Table 1**. Y2H-Gold strain bearing pGBKT7-ECD or CD of TLR4 vector were mated with Y187 strain bearing FetA-inserted pGADT7 vector. Yeast transformed with plasmids pGBKT7-P53 plus pGADT7-T or pGBKT7-lam plus pGADT7-T served as positive and negative controls, respectively. Growth was assessed on SD/−Ade/−His/−Leu/−Trp (quadruple dropout, QDO) plates incubated at 30 °C for 3 d.

Site-directed mutagenesis. A pCMV6-TLR4 construct containing 3.2 kb of mouse *Tlr4* gene (NM_021297) was purchased from OriGene Technologies. We used this vector as template for the generation of mutant plasmids with the help of the QuikChange site-directed mutagenesis system (Stratagene). We used SMART (simple modular architecture research tool; http://smart.embl.de/) and TollML (database of Toll-like receptor structural motifs; http://tollml.lrz.de/) web-based tools for the identification of leucine-rich repeats (LRRs) on TLR4. Forward and reverse primer sequences used for mutated TLR4 plasmid construction are listed in **Supplementary Table 2**.

[^{14}C] 2-DOG uptake. We incubated skeletal muscle cells or adipocytes with FFA in the absence or presence of FetA for 4 h followed by insulin (100 nM) stimulation for 30 min. [^{14}C] 2-DOG (0.4 nmol ml^{-1}) was added to each incubation 5 min before the termination of experiment. Cells were washed three times with ice-cold KRB buffer in the presence of 0.3 mM phloretin and then solubilized with 1% NP-40. [^{14}C]-2-DOG uptake was measured in a liquid scintillation counter (PerkinElmer Tri-Carb 2800TR).

Statistical analyses. We statistical analyzed the data by using a Student's unpaired *t* test or one-way analysis of variance, where the *F* value indicated significance; means were compared by *post hoc* multiple-range test. All values are mean ± s.e.m. *P* values < 0.05 was considered statistically significant.

37. Matthews, D.R. *et al.* Homeostasis model assessment: insulin resistance and beta-cell function from fasting plasma glucose and insulin concentrations in man. *Diabetologia* **28**, 412–419 (1985).
38. Li, W. *et al.* A hepatic protein, fetuin-a, occupies a protective role in lethal systemic inflammation. *PLoS ONE* **6**, e16945 (2011).
39. Lassenius, M.I. *et al.* Bacterial endotoxin activity in human serum is associated with dyslipidemia, insulin resistance, obesity, and chronic inflammation. *Diabetes Care* **34**, 1809–1815 (2011).
40. Lowry, O.H., Rosebrough, N.J., Farr, A.E. & Randall, R.J. Protein measurement with Folin phenol reagent. *J. Biol. Chem.* **193**, 265–275 (1951).
41. Dasgupta, S. *et al.* Mechanism of lipid induced insulin resistance: Activated PKCε is a key regulator. *Biochim. Biophys. Acta* **1812**, 495–506 (2011).
42. Dowler, S. *et al.* Protein lipid overlay assay. *Sci. STKE* **2002**, pl6 (2002).

doi:10.1038/nm.2851